TRIUMF Beam Physics Note
TRI-BN-18-XX
January 18, 2018

ISAC-I RF Acceleration

Olivier Shelbaya

TRIUMF

Abstract: This document provides an overview of the various components involved in ISAC-I postacceleration of radioisotope beams. A brief explanation of the operating principles and design features is given in a section by section manner.

4004 Wesbrook Mall, Vancouver, B.C. Canada V6T 2A3 Tel: 604 222-1047 Fax: 604 222-1074 www.triumf.ca

Contents

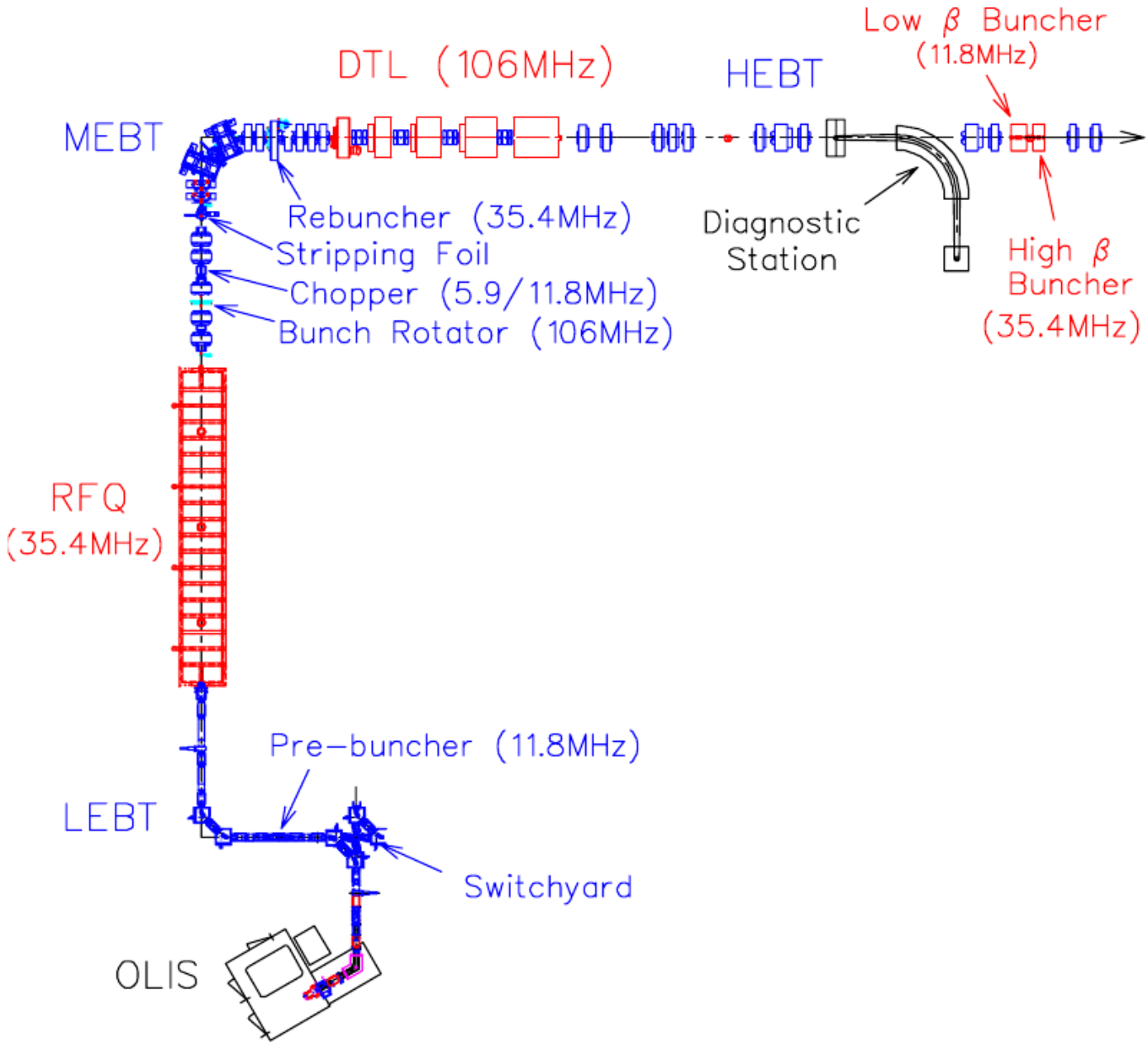

Figure 1: Overview of the ISAC-I RF accelerator system.

1 The Prebuncher & RFQ

The prebuncher is the very first RF element encountered by any accelerated beam. It consists of a set of parallel annular electrodes, with a 7mm aperture and an 8mm spacing[1], driven by an RF signal, which can reach up to $400V_{p-p}$[1]. The former is generated by summing up an 11.6MHz RF sinusoid and its two subsequent harmonics at 22.34 & 35MHz. The constituent harmonics must be phase-shifted such that their addition produces a composite waveform, approximating a sawtooth, as shown in Figure 2, which is fed into the plates.

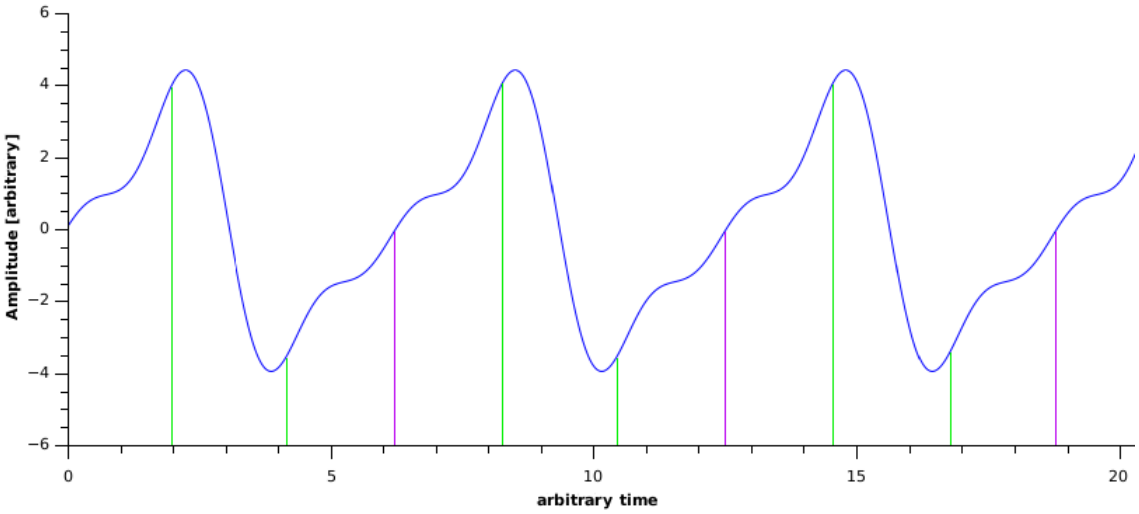

Figure 2: Representation of the prebuncher waveform, with the centroids for the main bunch in purple. Two 'empty' buckets, 35MHz apart, are highlighted in green for reference. The regions of maximum departure from a perfect sawtooth can be seen between t∼2-4, t∼9-11 & t∼ 15-17. RFQ output satellites arise mainly as a consequence of these nonlinearities.

As continuous beam flies through the prebuncher and encounteres its field, it is bunched into coarse buckets, separated by 86ns, or three 35MHz periods[2]. The main bucket is formed around the zero crossing point of the sawtooth waveform; ions crossing on the positive side are slowed down while on the negative side they are sped up, forming the main bucket. Two satellite pulses are also produced between each main peak, as a consequence of the nonzero fall time[3].

In all subsequent acceleration and bunching cavities, these bunches will remain coherent and intact. As such, the prebuncher is responsible for transitioning ion beams from continuous

[1] peak to peak voltage

[2] This is useful for experiments who measure the lifetime of metastable states, which may live up to a few ns long, as it ensures the next beam pulse arrives once all the generated events have elapsed.

[3] Consider a perfect sawtooth, with a perfectly linear slope and an instantaneous fall from its maximum positive to minimum negative value - in that case, all DC beam would get an RF kick which would be linearly inversely proportional to the difference in time from the zero crossing point. In the sinusoidal approximation, the linearity is only approximately true on either side of the main bucket zero crossing. All other points, particularly ones on the return slope from maximum to minimum, receive a substantial nonlinear kick. This causes some of the beam to be out of phase at the RFQ entrance.

to pulsed, so that all subsequent RF devices may act upon it.

Beam can now go through its first step in acceleration, accomplished by the RFQ. The device is unique in that it accomplishes two separate things simultaneously - the split ring, 4-rod structure, shown in Figure 3, both accelerates and focuses the beam through the 8m long structure. The RFQ design has the advantage of producing a large A/q acceptance, of $1 \leq A/q \leq 30$ [2], while not requiring any fine tuning of quadrupoles or RF cavities by operators - this has been calculated in the machine's design. The drawback is that the input energy, output energy and bunch structure are fixed, with $E_{in} = 2.04$keV/u, which must be set at the ion source, $E_{out} = 15$keV/u and an output bunch FWHM of $\sim$5ns [3], shown in Figure 4, on the right.

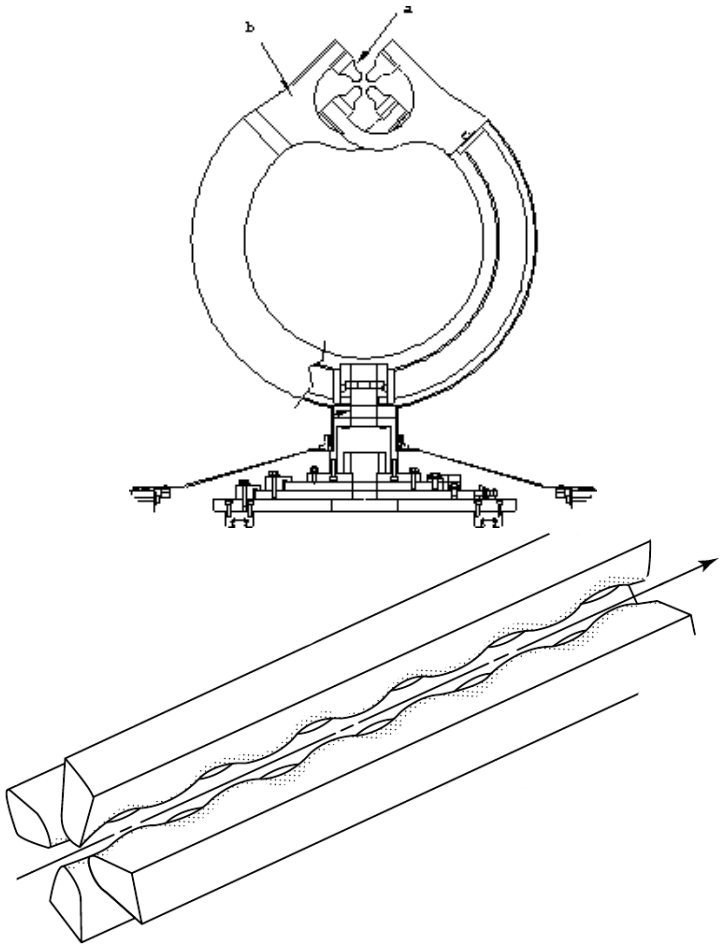

Figure 3: **left:** One of the split-rings of the ISAC RFQ - there are 19 in total - (a) RFQ electrodes (b) split ring support. **right:** schematic representation of the electrode 4-vane structure, which accelerates & focusses.

The prebuncher is designed to time focus the beam at the RFQ's entrance, 5.3m downstream [3]. The kick given to ions slightly off bunch centre is such that in the time of flight between prebuncher and RFQ, most ions contained in the region around the main bucket reference

point (purple line in Figure 2) will have sped up or slowed down, catching up together, and will form a time focus at the RFQ entrance. The energy-time phase space is shown in Figure 4, and the time-focus is the vertical feature on the left. This forms roughly 81% of the beam.

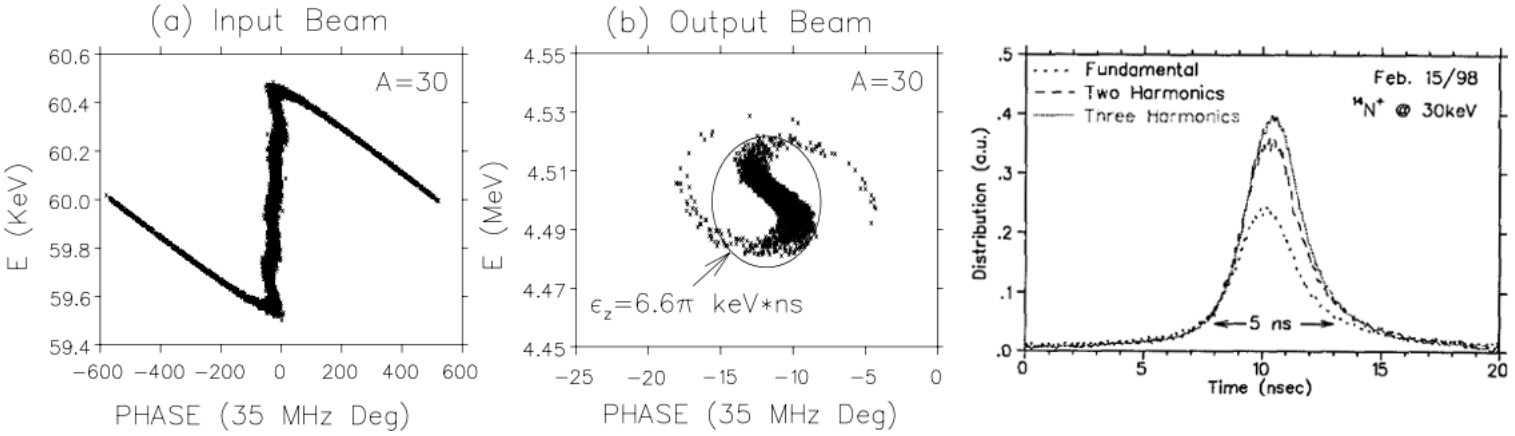

Figure 4: **left:** RFQ Longitudinal (energy-time) input emittance. The prebuncher's time focus is the vertical feature. **centre:** RFQ output longitudinal emittance. **right:** Output RFQ time spectrum.

The remaining 19% will not coincide with the main bunch at RFQ entry time, and will form the diagonal features found on either side of the main bunch, again visible on Figure 4. Of that beam, the parts which enter the RFQ at each vacant 35MHz period will form the satellites - this constitutes 3.5% of the total beam. Since these small amounts of beam enter precisely at the start of an RF cycle, they will be accelerated by the RFQ and transmitted. Finally, the remaining 15% of these side structures will enter the RFQ out of phase, and will follow an irregular trajectory across the accelerator, until they either collides with the 4-vane, the RFQ walls, or will exit the RFQ unaccelerated[4]. The output phase space of RFQ accelerated beam is shown in Figure 4, in the centre.

By time focussing, one ensures that bunched beam travels through the RFQ's accelerating structure coherently in time and therefore suffers the same intrinsic increase in energy spread[5] and by bunching instead of chopping, known as *phase concentration*, one increases overall transmission[6][4]. The prebuncher also defines to the RFQ's energy acceptance, allowing for a beam with a gaussian distributed energy of σ = 10eV[7] In other words, the prebuncher RF field is sufficiently powerful to slow down or speed up particles that have up to 10eV variation from the bunch centre. Particles with a larger energy spread will not be time focussed with the main bunch by the time it reaches the RFQ.

[4] only an extremely small amout actually exits the RFQ. Most of the 19% hits the walls.

[5] if the bunch entering the RFQ is poorly time focussed, the RF acceleration will only worsen the time spread.

[6] since chopping involves throwing away most of the beam that isn't in the buckets.

[7] for example this means an OLIS beam with charget state 1+ can have a bias voltage error of ± 10V, 2+ can have ± 20V, and so on..

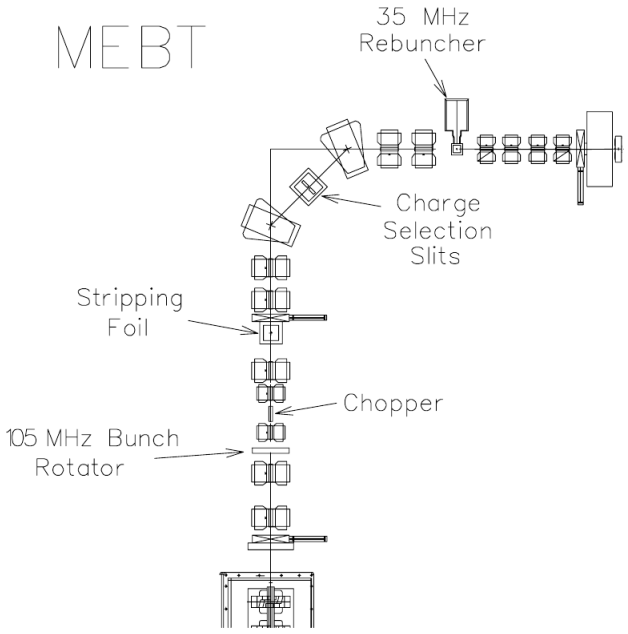

Figure 5: MEBT section overview.

In all, the prebuncher-RFQ pair accepts a continuous, low energy ion beam, shapes it into RF buckets and accelerates them up to 153keV/u, multiplying beam energy by a factor of ∼75.

2 MEBT

Pulsed beam exiting the RFQ at 0.153MeV/u can satisfy the low energy tail of scattering experiments, however many require energies that are significantly higher. To accelerate in the MeV/u range, pulsed beam must undergo some transformations. The MEBT section is dedicated to prepare pulses for further acceleration and bunching.

To acheive this, it may be necessary to increase the charge state of the pulsed beam, which in turn will lower the voltage requirement for supplemental accelerating cavities. This is accomplished by a carbon stripping foil [5], intended to bump the mass-to-charge ratio into the $2 \leq A/q \leq 7$.

The MEBT section is thus composed of three subsections:

1. Entrance matching to stripping foil
2. Charge selection corner
3. Exit matching into DTL

2.1 MEBT Entrance Matching

Pulsed beam exiting the RFQ still possesses a finite timebunch spread, shown in Figure 6, on the top left. To minimize beam divergence effects caused by the stripping foil, the first 5 MEBT quadrupoles provide x-y focussing on the foil surface, while a three-gap bunch rotator provides a time focus on the foil [1]. The goal is for each bunch to hit the foil in as short an amount of time possible, on as small of a point as possible.

Beam interacting with the stripping foil will cause overall divergence due to scattering, represented in Figure 6, on the top-left. Spatially[8] focussing the beam on the foil will help minimize the increase in emittance. Considering the interaction in energy-time phase space, the foil will introduce a finite invrease in energy spread. This is shown in Figure 6, on the bottom left. Given this finite ΔE, and considering that the energy-time phase space area of a beam is a conserved quantity in RF acceleration processes[9], then it is apparent that to minimize the increase in phase-space area, it is necessary to time-focus the bunch at the foil - graphically represented in Figure 6, on the bottom left. This is accomplished by the bunch rotator[10].

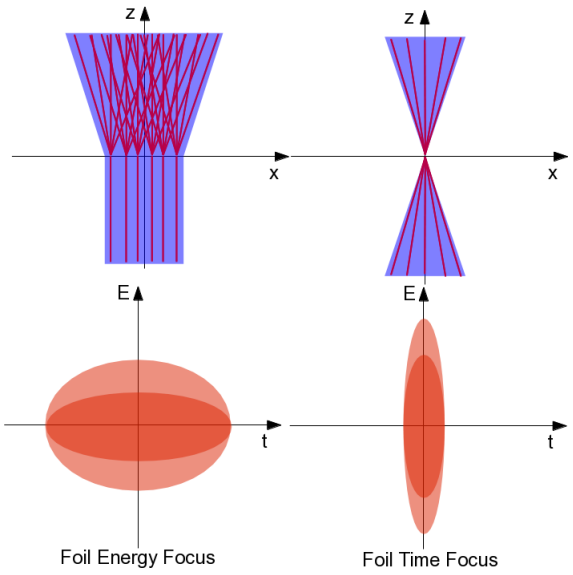

Figure 6: Effects of stripping foil on beam geometry, for z being the beam axis and x being transverse (also valid for y). Note the increase of emittance for the unfocussed case - each point on the foil surface can be considered a point source of beam, which complicates beam transport downstream.

[8] spatial (x-y) focussing is also commonly referred to as transverse focussing

[9] As the energy-time phase space area increases, this also means the beam velocity and position spreads increase, translating into a decreased ability to bunch and focus, which ultimately kills transmission.

[10] Since the RFQ-Bunch rotator-stripping foil distance always remains fixed, and since the RFQ output energy (in keV/u) remains constant (and considering that different mass beams will exit the RFQ with a minuscule velocity difference), in order to time focus on the stripping foil, the bunch rotator RF phase must remain constant as well, equal to 143.2°. Only the RF amplitude has to vary, proportional to A/q. Significantly moving this phase will affect the time focus quality on the foil and will lead to extra beam losses beyond.

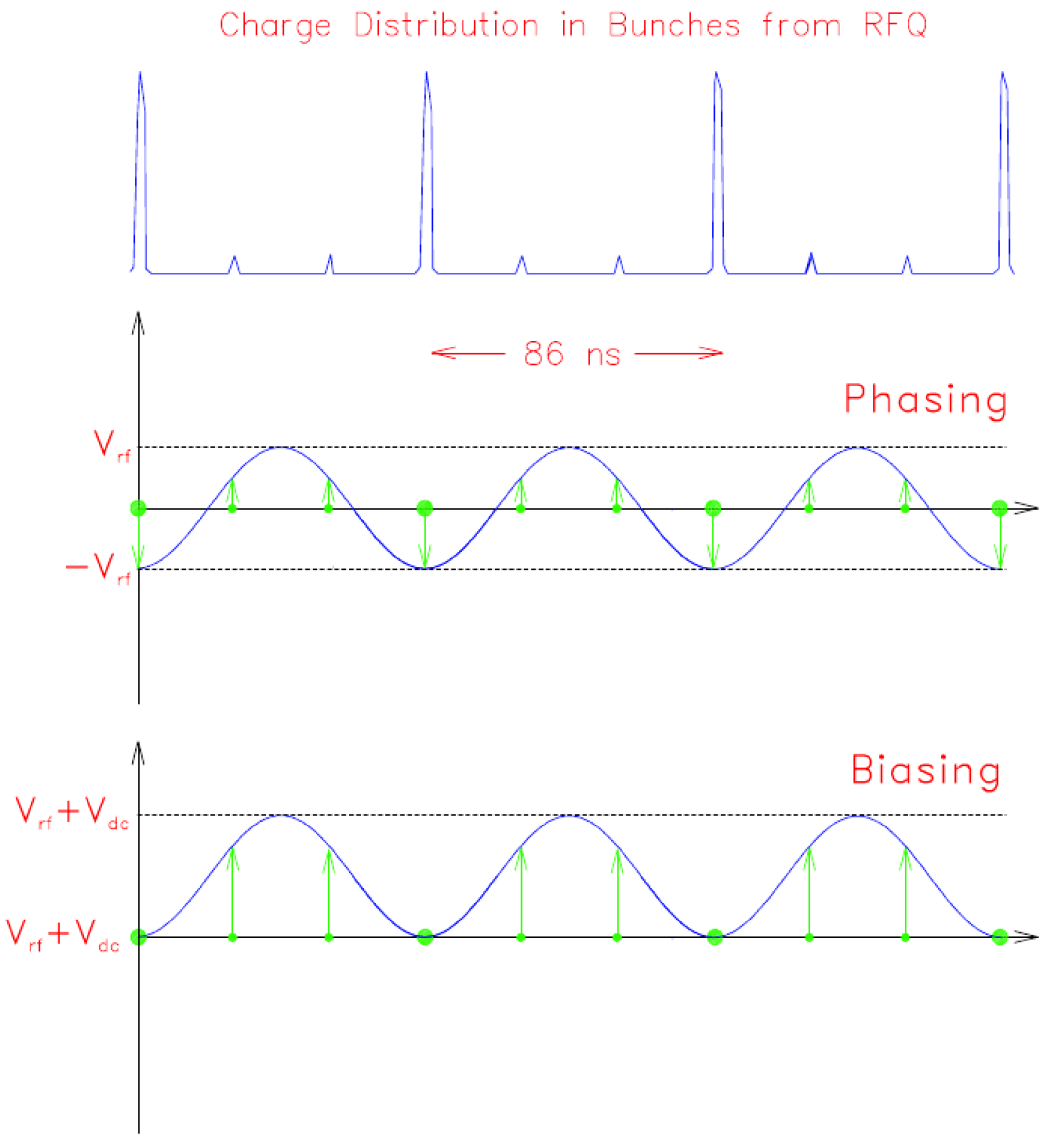

Figure 7: Energy-time (longitudinal) phase space of beam before (dark red) & after (light red) foil interaction. **right:** Schematic representation of the main buckets and both satellites. The 11MHz chopper RF is shown in the centre graph, and the chopper RF + chopper plate DC offset is shown at the bottom. Note that the deflection field is 0 when the main bunch crosses the buncher.

Both the main bucket and the satellites fly through the bunch rotator, since they are synchronous with the 35MHz main RF. Two out of every three buckets remain undesired. To provide experiments with a 'clean', 86ns periodic ion pulse, the next step is to remove the unwanted satellites. This is accomplished by the dual frequency chopper, which is composed of two pairs of parallel plates, driven at 11.8MHz and 5.9MHz (half the frequency), in addition to a 2mm slit located 1.35m downstream [6]. Running the 5.9MHz plate will

only allow one out of every other main bunch to transmit to experiment, and it is seldom used as of 2015.

The chopper's operation principle is demonstrated in Figure 7, on the right. By coupling the 11.8MHz RF waveform with a large DC offset voltage[11], only the main bucket is allowed to pass through the 2mm slit, while both satellites are deflected by the RF electric field onto the plate. This is because the addition of DC offset and RF voltage is phased to produce zero deflecting field as the main bucket flies through.

A convenient byproduct of this setup is the ability to monitor beam presence during delivery, using the satellites as a proxy, as done by the ISAC Current Monitoring System. For these purposes, the chopper RF phase is tuned to acheive the same degree of deflection on both satellites. To accomplish this, one searches an RF phase to produce the timing shown on Figure 7 on the bottom right, in which both satellites are symetrically located on either sides of an RF crest. This ensures both bunches will hit the same point on the chopper plate.

Pulsed beam exiting the RFQ has now been time-focussed on the stripping foil by the Bunch Rotator, positionally focussed on the foil by the MEBT quads, and the unwanted satellites have been deflected by the chopper, onto the chopper plate, and used as a proxy for beam monitoring.

2.2 MEBT Charge Selection

Charge-exchange (stripping) with the carbon foil will generate a distribution of charge states. These states exit the stripping foil having lost a slight amount of energy due to the ionization process in the foil, up to $\sim$ 3keV/u. This can be seen by examining the Bethe formula[12], which governs energy deposition by energetic particles in thin foils:

$$-\frac{dE}{dx} \propto Z_P^2 \frac{Z_T}{A_T} \tag{1}$$

In other words, the rate of energy loss is proportional to the total atomic number of the incident particles Z_P squared and the ratio of target atomic number Z_T and mass number, A_T. In our case the stripping foil is usually carbon[13] so Z_T/A_T can be considered a constant. Concretely, this means that heavy beams will lose more energy than light beams. Knowing this is useful for tuning elements downstream, particularly when it comes to adjusting tunes when scaling from one species to another.

[11] typically around 1.5 to 2kV - this corresponds to MEBT:CHOP:HIGH (11MHz) in EPICS
[12] charge exchange efficiency can also be inferred by using this formula.
[13] aluminium, tungsten, diamond sheet and gold sheet are other possible materials, among others.

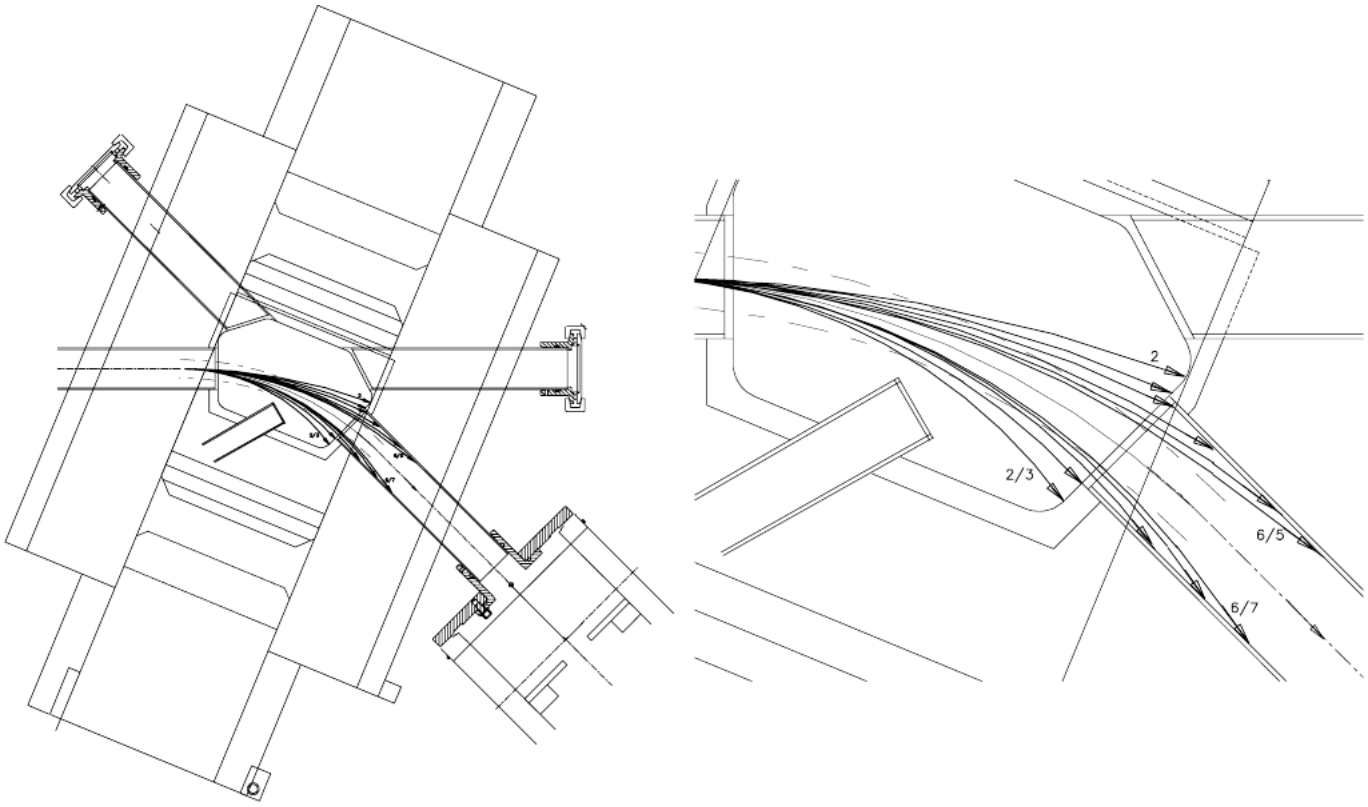

Figure 8: Representation of the first MEBT dipole magnet (L) and zoomed in view (R). The trajectories for several A/q's have been plotted to demonstrate the magnetic field effect on trajectories and the resulting charge state filtration/selection. The slits can be seen on the left figure, at the bottom right.

All generated charge states exit the foil region travelling along the beam axis. To clean things up and select the appropriate charge state, two bending magnets on either side of a set of charge selection slits, defining a 90° corner are used. Most charge states will fly through MEBT quadrupoles 6 and 7, and enter the first MEBT bending magnet [1].
If we consider the Lorentz force law:

$$\vec{F} = q(\vec{E} + \vec{v} \times \vec{B}) \tag{2}$$

Considering the Bethe equation's atomic number (a proxy for mass) proportionality, one can see how for a heavier beam (higher Z), more energy will be lost in the foil, resulting in a reduced velocity $\vec{v}$. To acheive the same deflective force (per unit nucleon) with the MEBT benders, one must therefore increase $\vec{B}$. This is particularly useful to remember when scaling tunes or switching from one species to the next - not only must the dipole fields be changed to accomodate the different A/q, but a small correction must also be supplied by the operator to compensate for the differential energy loss variation in the stripping foil.

Stripping foil integrity (and constant performance) is thus a very important consideration for beam delivery. As the integrated foil current goes up, the likelyhood of foil property variations increase. After a certain integrated current, the foil will fail. To compensate for

slow, slight changes in foil thickness/energy loss, an RF global phase adjustment option is available. Considering the example where foil thickness decreases over time, this means that dE/dx will decrease as well, resulting in a decreased time of flight until the next RF element.

Phase shifting the 11MHz master frequency for upstream elements by 1° for a 12C beam at 0.153MeV/u means the timebunch centroid will be positionally shifted by ∼1.3mm per 11MHz RF period. Ignoring higher order/nonlinear effects, and simply considering a bunch centroid position offset of 1.3mm crossing an RF gap with a field gradient of 7.5kV/cm[14], this means the bunch centroid would see a peak voltage difference of ∼975V when crossing the RF field. Using the same rule of thumb argument, a 5° global phase shift would result in a first order position difference of ∼6.5mm per 86ns, and cause a ∼4.875kV peak RF field difference, which is a significant value, especially when crossing several sequential RF cavities.

2.3 MEBT Exit Matching

The second dipole magnet then aligns the charge selected beam into the final mebt subsection, which is dedicated to matching beam into the DTL. The position focus is again accomplished by the present MEBT quads, while the charge selected bunch is time focussed at the entrance of the first DTL cavity, for exactly the same reasons as with the RFQ: the minimization of bunch timespread means less increase in overall emittance during acceleration.

Time focus at DTL tank 1 is accomplished by the 35MHz MEBT Rebuncher. There are two important parameters to accomplish a proper focus - the RF amplitude and its phase. The RF amplitude will vary with A/q, requiring higher voltage setpoints for higher A/q values, while the phase must be manually tuned to coincide with bunch passage through the buncher cavity. Changes in energy can be diagnosed with the Prague magnet downstream - if one drifts beam through the DTL (RF off), finds its energy on the Prague, then turns on the rebuncher, then setting its phase to obtain the same prague average energy means the rebuncher is properly phased. [15].

At this point, continuous beam has been modulated by the prebuncher and accelerated to 153keV/u by the RFQ. Clean output bunches with appropriate A/q exits the MEBT section being transverse focussed by the final MEBT quads, and time focussed at the entrance of DTL Tank1 by the MEBT Rebuncher, ready for further acceleration.

3 Prague Magnet

Before discussing the final step in ISAC-I acceleration, it is useful to describe the diagnostic section that lies beyond it. Since the RFQ produces an output beam of known energy, and the MEBT section has been designed with this specification in mind, no precise energy measurement was required throughout MEBT. Successful transmission served as a proxy

[14] roughly the values for the MEBT rebuncher

[15] Since there are no fast faraday cups immediately downstream of of the rebuncher, or any fast beam profiling electronics until well after the DTL, transmission through the DTL versus rebuncher phase is used to diagnose the phase timing. If the rebuncher phase is correct, bunches will receive zero average energy (explained in next section), whereas if the rebuncher is improperly phased, energy will either be given or taken away from bunches, which will affect the energy and time of flight through the DTL

for beam energy spread. However, once we enter high-energy beam transport (HEBT), with further acceleration with a variable energy linear accelerator, being able to precisely measure the output energy spectrum becomes critical. For this purpose, a 90° analyzing magnet, with a radius of curvature $r = 1.537$m [7] is installed downstream of the final linear accelerator.

The air-cooled[16] analyzing magnet is used to precisely measure the output beam energy. The Prague [17] is located symetrically between two slits, which optically define an object and an image. In other words, given the Prague's field, if beam is focussed at the object slit, and flies through the Prague, it will emerge focussed at the image slit.

However, the Prague is only able to acheive a horizontal focus (x-plane). It is thus necessary to adjust upstream HEBT quadrupoles for beam to be slightly convergent at the object slit, in order to keep beam acceptably small through the magnet.

Beyond the dipole is a diagnostic box containing a harp scanner with 15 wires, spaced by 0.8mm, a Faraday cup and a silicon detector [8]. Since the Prague magnetic field $\vec{B}$ is known, as well as its radius, then transmitting the Prague immediately gives us information about beam energy. Looking at equation 2, if we set $\vec{F}$ equal to centripetal acceleration, we obtain the cyclotron formula, which can be re-arranged in terms of energy, for a given A/q:

$$E = \frac{1}{2}\frac{r^2 B^2 q^2}{2A^2} \tag{3}$$

Using reference calibration values, it is possible to infer the output energy for a beam of given A/q, with prague field B (in gauss) by taking the ratio of energies:

$$E = \left(\frac{EA^2}{B^2q^2}\right)_{ref}\left(\frac{B^2q^2}{A^2}\right) \sim \frac{1.405 \cdot 10^{-6} B^2}{(A/q)^2}[MeV/u] \tag{4}$$

Knowing the spacing of harp wires, measuring the beam spread on the former gives information about the energy spectrum. Considering equation 3, taking a ratio of energies corresponding to two different radii of curvature, we find that a distance d, corresponding to the difference between r_1 and r_2, is related to energies E_1 and E_2 by:

$$d = r_2\left(1 - \sqrt{\frac{E_1}{E_2}}\right) \tag{5}$$

knowing this, we can infer that the energy spread will be:

$$\Delta E = E\left[\left(\frac{d + r_2}{r_2}\right)^2 - 1\right] \tag{6}$$

knowing that the distance between two harp wires is 0.8mm and that the Prague radius is 1.537m, this means that the energy spread between two adjacent harp wires is roughly equal to 0.1% of the average bunch energy. Also, since the harp has 15 wires, this effectively corresponds to an energy acceptance of $\sim 1.5\%$ total beam energy, meaning it presents a very narrow window of observation. While tuning the beam on the harp, care must thus be taken not to 'lose' beam by varying the Prague field too quickly.

Knowing the above, it is not necessary to use the silicon detector to characterize the energy spectrum. The latter, however, is currently used to characterize beam composition, as it is

[16] don't forget to turn it off
[17] as it is nicknamed

sensitive to total energy, unlike the harp which has a ∼15keV total acceptance. The silicon detector can therefore detect similar A/q contaminants in the beam, which the harp would miss.

4 The Drift Tube Linac

The ISAC DTL can output bunched beams from 0.153 to 1.8MeV/u [9] for $2 \leq A/q \leq 7$. It consists of 8 RF modules - 5 tanks interspersed with quadrupole triplets and, with the exception of the tank4-5 gap, RF bunchers used to time focus into the next RF cavity.

The operating principle of the DTL is simple: regardless of their velocity, accelerated bunches must spend equal amounts of time drifting through tubes where they feel no electric field, thus no acceleration. The shape of cavities emerges as a consequence of this requirement: tube length is adjusted such that at each gap crossing, bunches see the same accelerating gradient generated by the sinusoidal RF field. As particles gain in velocity, tubes must get longer to maintain constant drift time.

The ISAC DTL acceleration tanks (1-5) are known as interdigital H-mode[18] (IH) tanks. This can be understood by looking at Figure 9, on the right. The drift tubes contained in each tank are sequentially anchored to the top and bottom of the cavity, with both sets being 180° out of phase with each other. In other words, when one set of interdigital tubes are at +V, the other is at -V, producing the accelerating gradient.

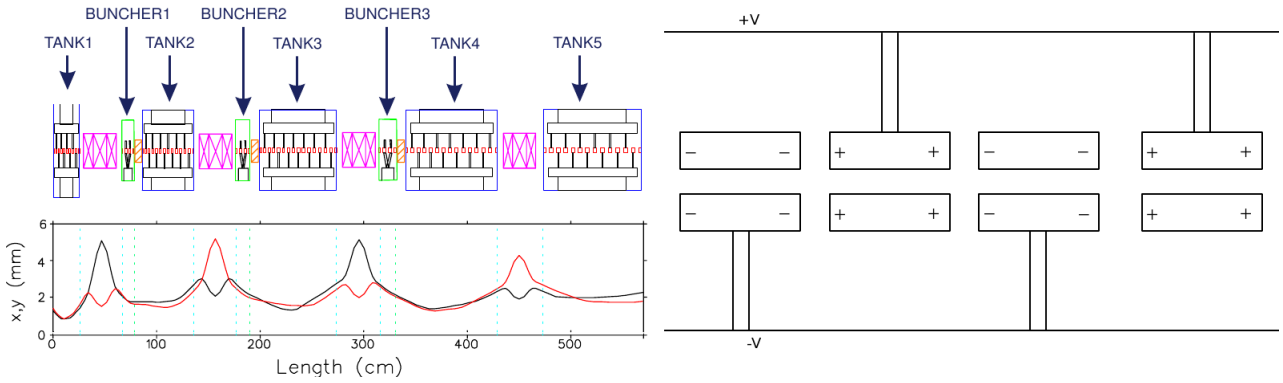

Figure 9: **left:** Overview of the DTL with tanks & bunchers highlighted. Transverse beam profile dimensions are shown at the bottom. Notice how the x and y profiles alternatively defocus exiting each tank (before being corrected by the quads) - by Tank5 output both dimensions have been smoothed out to ∼2mm radius. **right:** Schematic representation of the interdigital drift tube tank layout, showing instantaneous charge at the crest of an RF sinusoid - adjacent drift tubes have equal but opposite charge, producing the accelerating gradient. Note that particles feel no electric field at all while drifting through a tube. Also note that in the ISAC DTL, not all interdigital tubes share equal length, even within a tank.

[18] H-mode referes to the magnetic field $\vec{H}$ being parallel with the beam axis, and the electric field being transverse (x-y).

[18] this can be understood by considering that while drifting in a tube, a particle will feel the same charge

Looking at a sinusoid, there are two regions of interest for DTL operation: the synchronous (or 0°) phase and the bunching (or -90°) phase. For the first case at 0°, positively charged bunches emerge from a tube just before the charge of the tube reaches its positive maximum, with the next tube at equal but negative potential. This produces a repulsive electric field gradient, producing a finite energy gain for the bunch. However, given a finite bunch time width Δt, this also means that the front and rear ends of the bunch will see identical sides of the RF sinusoid, as the RF field reaches its maximum and begins to decrease. Consequently, 0° phasing produces maximum acceleration and no bunching.

Conversely, the -90° bunching phase is timed such that as the bunch emerges from one tube, the RF field transitions from negative to positive[19]. More energetic (higher velocity) particles exiting first feel a slightly negative electric field, slowing them down. The bunch center crosses the gap at 0 net field. Late (slower) particles enter the gap as the electric field slightly positive, causing them to gain energy. This cavity phasing is known as a *pure buncher*, as it produces no net acceleration. It only reduces the time spread of exiting bunches.

The dynamics of RF bunching may be visualized by considering the energy-variation vs ϕ_{RF} phase space diagram for an idealized adiabatic[20] linear accelerator. The energy variation for a given particle, ΔW, is measured with respect to a *synchronous* particle, which is in the centre of the bunch, and has the average energy of the bunch. Such plots are shown in Figure 10, for intermediate phasing and -90° phasing.

Particles located anywhere within the Stable-Unstable separatrix[21] will run parallel to the adiabatic lines. The stable area within this line is known as the bucket, and defines the core of the ion bunch - particles within this line will remain bunched, while those outside the line will eventually diverge and fall out of the bunch[22]. This is a consequence of the RF bunching caused by running the cavity at $\phi_S < 0°$. As the bunch crosses several gaps, it progressively rotates counterclockwise.

Notice the acceptance difference between the left and right examples in Figure 10. While pure -90° bunching (right) produces a broad and symmetric phase space bucket, spanning $\sim$360°[23] while accelerating produces a narrower, $\Delta\phi \sim 40°$ asymmetric bucket. This highlightes the importance of time (phase) focussing into accelerating tanks, which is why DTL bunchers are contained between tanks 1-3[24].

---

from all directions, therefore there is no charge gradient, and thus no field. This condition fails close to the tube edges, and the result is a fringe electric field, which will defocus the beam.

[19] only negative to positive phasing works. positive to negative would only speed up fast particles and slow down stragglers, causing an overall increase in time spread.

[20] adiabatic means no transfer of energy, which is approximately true if the gaps provide a small increase in energy compared to the total particle energy.

[21] the separatrix is the line that defines the bunch in phase space.

[22] as particles diverge from the bunch, both in time and space, they eventually hit the RF wave at an incoherent time, and are lost

[23] this phase (time) acceptance will vary with cavity design

[24] DTL Tank 5 can accelerate beam to higher energy than 1.5MeV/u - around 1.8 as maximum. However, by the time beam exits tank 4, it has a sufficiently narrow time (phase) spread that tank 5 can be used to both accelerate and bunch to 1.5MeV/u.

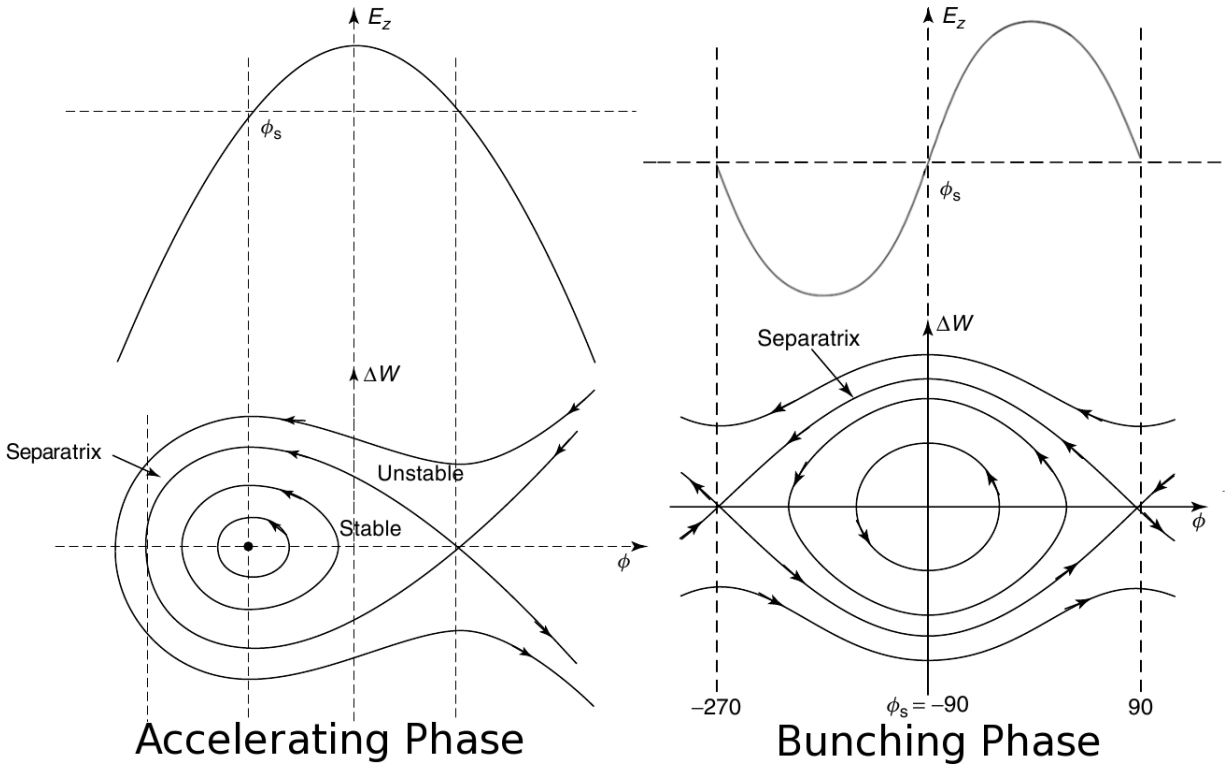

Figure 10: **left:** The Fish - comparison of RF electric field variation (top) RF cavity energy-phase phase space, for a cavity phased at some intermediate ϕ_S ¡ 0°. On the bottom figure, the lines represent paths that particles will follow due to the bunching effects of the RF. ΔW represents change in energy from the bunch average, which is a proxy for velocity. Notice how when ΔW exceeds a certain value, the trajectory is unstable - meaning the particle will in time, diverge from the bunch. The stable particle, with ΔW (thus Δv) = 0, receives no change in velocity. A hypothetical bunch, would cross several cavity gaps, receive acceleration by the RF, and rotate counterclockwise within the Stable separatrix, with the phase-space area remaining unchanged. **right:** The same diagram, but for a cavity phased at -90°, showing a pure buncher.

As RF acceleration through the tank structures tends to transversely defocus the beam, the DTL quadrupole triplets are set to acheive a *waist* in the middle of the next acclerating tank. This can be seen by inspecting Figure 9, on the bottom left[25]. Given the combination of strongly focussing quadrupole triplets and the close succession of independantly phased RF cavities with time-varying fields, which themselves have a defocussing effect, it should come as no surprise that the DTL has a strong sensitivity to beam profile and alignment. Great care should be taken throughout a setup to ensure optimal beam alignment, cross section, focus and MEBT output time-structure.

One can the see that, for -90° bunching, the average energy given to the bunch is zero - integrating for times between early and late particles, the average field is 0. For 0° bunching,

[25]While setting DTL tanks, one will find that as tank amplitude is being increased to produce the desired E_{out}, it is periodically necessary to change the DTL quad values to maintain transmission. When transmission starts to fall as the RF amplidue rises, this is because RF defocussing is getting stronger than quadrupole triplet focussing.

the average between early and late particles, assuming a symetrically centered bunch on an RF crest, will be just below the maximum value of the RF field[26]. Conversely, phasing the bunch anywhere between -90° and -180° will go from pure bunching, to bunching with average energy loss (deceleration), to pure deceleration, without any bunching.

In the case of the ISAC DTL, accelerating tanks (1 to 5) are procedurally phased just below 0° (say -2° or -3° [27]) for maximal ΔE with a small amount of bunching, to make the spectrum appear subjectively *nice*. This corresponds to the region of strong E(ϕ) slope on Figure 11, on the right.

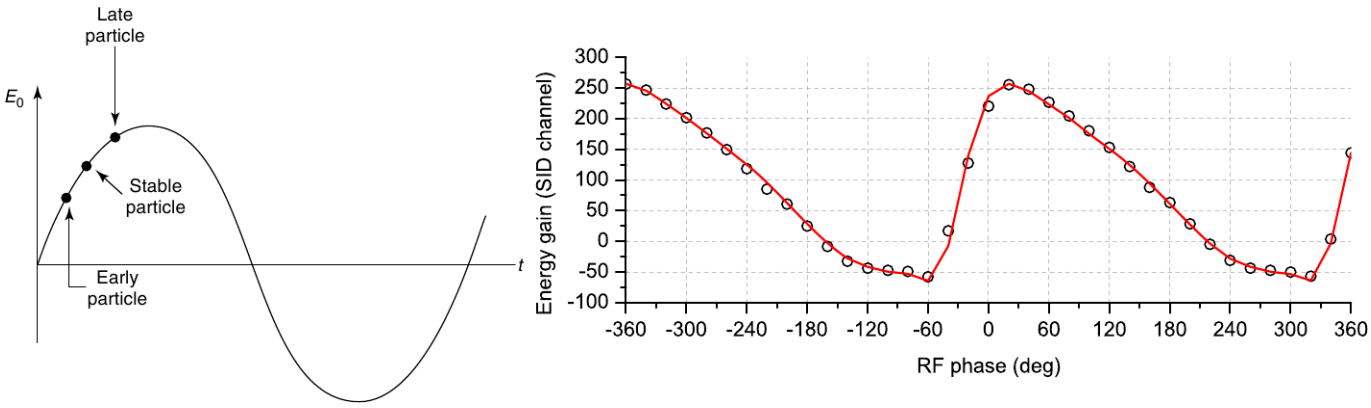

Figure 11: **left:** representation of an RF sinusoid, highlighting an example of bunch phasing - in this case, with ϕ ∼-45°, pulsed beam is being both bunched and accelerated. **right:** bunch energy gain vs RF phase for DTL Tank1 - notice how the coherent bunching regime (from pure bunching to pure acceleration) produces a sharp slope for ΔE(ϕ), while all other phases produce a much weaker energy response. Needless to say, the energy spectrum for all phases not within the strong slope region produce a messy output energy spectrum, since no coherent bunching takes place.

Since the DTL tanks operate separately from one another, to acheive variable energy output, downstream tanks are turned on/off to acheive coarse energy selection, and the RF field intensity is adjusted in the last active tank to acheive fine energy selection. Intertank bunchers are phased at -45°, to provide some acceleration while bunching [10]. In the case that maximum energy is reached prior to the last buncher (buncher 3), the former is phased at -90° to acheive a minimized output time spectrum.

Finally, refering back to equation 6, Table 1 shows the expected output energy spectra for optimally tuned beams, at various energies. Assuming proper Prague and HEBT quad field settings, the expected harp spectrum width is shown on the right.

[26] this is a mathematical consequence of having a constantly varying electric field, and is represented by the transit-time factor (TTF), which is the ratio of effective acceleration by a time-dependant RF field, divided by the ideal case of a time independant, constant cavity gap voltage.

[27] this corresponds to hunting the point on the prague harp when the beam profile stops moving to the left and begins moving to the right - this corresponds to crossing over the crest of an RF sinusoid in Figure 11.

Cavity	Energy [MeV/u]	Approx. Prague Harp Width [wires]
RFQ	0.153	7-8
Rebuncher	0.153	11-12
Tank 1	0.238	7-8
Buncher 1	0.254	7-8
Tank 2	0.439	7-8
Buncher 2	0.461	6-7
Tank 3	0.781	6-7
Buncher 3	0.803	6-7
Tank 4	1.149	5-6
Tank 5	1.530	3-4

Table 1: Expected Prague harp energy spectra for various configurations. Note: all previous cavities are assumed to be on and properly tuned.

5 Summary

With all of the above taken into consideration, the room temperature ISAC-I accelerator system accepts continuous ion beams with $2 \leq A/q \leq 30$, including short lived radioactive beams, and offers experiments beams ranging from 153keV/u to ¿ 1.5MeV/u, for a variety of charge states satisfying $2 \leq A/q \leq 7$. These are delivered in 86ns periodic pulses, with the option to double the period to 172ns (but halve the transmission), should it be required. Output bunches will have energy spreads below 0.8%.

These energies are ideal for elastic scattering and nuclear astrophysics, which investigate the production of metastable exotic isotopes and their isomers via resonant energy collisions. For each isotope, there are many energy channels at which these reactions take place, so it is ideal to have a variable energy output accelerator system, which can be fine tuned down to the keV level, providing experiments with the ability to investigate several closely spaced channels in a short timespan.

References

[1] Mitra, A.K., *TRIUMF Design Note 01-14 - RF Structures For The TRIUMF-ISAC Facility*

[2] Koscielniak, S., *Beam Dynamics Studies on The ISAC RFQ at TRIUMF*

[3] Laxdal, R.E., *Completion And Operations of ISAC-I And Extension to ISAC-II (2001)*

[4] Koscielniak, S., *et al.*, *Beam Dynamics of the TRIUMF ISAC RFQ*

[5] Laxdal, R.E., *TRIUMF Design Note 99-27 - Charge Distribution and Beam Loss after MEBT Foil*

[6] Marchetto, M., Rawnsley, W.R., *TRIUMF Design Note 08-22 - The MEBT chopper as ISAC-II intercepting current monitor*

[7] Laxdal, R.E., *TRIUMF Design Note 00-29 - Commissioning Preparation and Test Results*

[8] TRIUMF, *Annual Report Scientific Activities, 2001.*

[9] Marchetto, M., *et al.*, *Upgrade of the ISAC DTL Tuning Procedure at TRIUMF.*

[10] Laxdal, R.E., *et al.*, *TRIUMF Design Note 97-4 - The Separated Function Drift Tube Linac for ISAC*